Is it Possible to Quantify Irrigation Water-Use

by Assimilating a High-Resolution Soil Moisture Product?

Ehsan Jalilvand[1], Ronnie Abolafia-Rosenzweig[3], Masoud Tajrishy[4], Sujay V Kumar[5], Mohammad Reza Mohammadi[4], and Narendra N Das[1,2]

[1]Biosystem & Agricultural Engineering, Michigan State University, Michigan, USA

[2]Civil and Environmental Engineering, Michigan State University, Michigan, USA

[3]Research Applications Laboratory, National Center for Atmospheric Research, Boulder, USA

[4]Civil and Environmental engineering, Sharif University of Technology, Tehran, Iran

[5]Hydrological Sciences Laboratory, NASA Goddard Space Flight Center, Greenbelt, MD, USA

Corresponding Author: Narendra N. Das (dasnaren@msu.edu)

Abstract

Irrigation is the largest human intervention in the water cycle that can modulate climate extremes, yet global irrigation water use (IWU) remains largely unknown. Microwave remote sensing offers a practical way to quantify IWU by monitoring changes in soil moisture caused by irrigation. However, high-resolution satellite soil moisture data is typically infrequent (e.g., 6 -12 days) and thus may miss irrigation events. This study evaluates the ability to quantify IWU by assimilating high-resolution (1km) SMAP-Sentinel 1 (SMAP-S1) remotely sensed soil moisture with a physically-based land surface model (LSM) using a particle batch smoother (PBS). A suite of synthetic experiments is devised to evaluate different error sources. Results from the synthetic experimentation show that unbiased simulations with known irrigation timing can produce an accurate irrigation estimate with a mean annual bias of 0.45% and the mean R^2 of 96.5%, relative to observed IWU. Unknown irrigation timing can significantly deteriorate the model performance by increasing the mean annual bias to 23% and decreasing the mean R^2 to 36%. Adding random noise to synthetic observations does not significantly decrease model performance except for the experiments with low observation frequency (>12 days). In real-world experiments, the PBS data assimilation approach provides a mean bias of -18.6% when the timing of irrigation water use is known. This underestimation is possibly attributable to missing part of the irrigation signal. Yet, significantly

higher irrigation was estimated over the irrigated pixels compared to the non-irrigated pixels, indicating that data assimilation can skillfully convey irrigation signals to LSMs. LSM calibration provides a 10% improvement to soil moistrue RMSE relative to the open-loop simulation. PBS data assimilation provides an additional 50% improvement to simulated soil moisture RMSE by correcting the model state and superimposing the optimal (unmodeled) irrigation on precipitation forcing.

Keywords: Irrigation water use, high-resolution soil moisture, Particle batch smoother, SMAP, Sentinel 1, data assimilation

Highlights

- Complex human irrigation decisions can be modeled using the PBS approach
- Irrigation can be estimated accurately by assimilating a weekly high-resolution SM data containing the irrigation signal
- Instead of using an irrigation module in the LSM, PBS can be used to account for irrigation

Introduction

Agricultural production is projected to require a 70% expansion by 2050 as a result of population growth, climate change, and dietary shifts towards water intensive products associated with increasing incomes (FAO, 2009, Tilman et al., 2015). Food production is mainly sustained by irrigation (Jägermeyr et al., 2015), which is by far the largest consumer of freshwater resources globally (Döll & Siebert, 2002). However, the planetary limit for freshwater withdrawal is quickly approaching (or already exceeded) in many parts of the world (Steffen et al., 2015). Moreover, it is expected that part of the irrigation agriculture water be re-allocated to higher productivity sectors in the near future (World Bank, 2020). Thus, authorities seek to limit agricultural water consumption globally. However, a key requirement to enforce any regulation is monitoring the water withdrawn by the farmers (Foster et al., 2020). Monitoring groundwater storage changes through GRACE satellite observations has revealed significant depletion in major aquifers across the globe (Scanlon et al., 2012, Joodaki et al., 2014, Frappart at al., 2018), mainly due to unsustainable water withdrawal (consuming more water than received from rainfall) for agriculture (Doll et al., 2015). Thus, quantifying Irrigation water use (IWU) is a valuable component for optimal management of depleting surface and groundwater resources to sustain crop production (Abbot et al., 2019).

Despite the importance of monitoring agricultural water use, much of the water withdrawn for irrigation is unmetered due to the high installation and mainte-

nance costs of required ground sensors (Wells, 2015). For instance, in the US less than 36% of wells are equipped with a flowmeter (Foster et al., 2020) and the fraction is much less in the developing countries where smallholder agriculture is the common practice (Wester et al., 2009; Shah, 2014). Even when an in-situ metering network is in place, there is usually a large gap between the formal policies and the local practices. Farmers are reported to adopt tactics to circumvent existing limitations such as illegal surface water diversion, drilling unlicensed wells, or tampering with meters installed on legal wells (al Naber & Molle, 2017; Balasubramanya & Stifel, 2020).

Satellite observations provide a unique opportunity to monitor irrigation and address many of the above-mentioned issues with in-situ measurements. Thermal and optical sensors can measure evapotranspiration (ET) using crop coefficients obtained from satellite-based vegetation indices (Allen et al., 2005; Farg et al., 2012) or surface energy balance that is highly correlated with irrigation (Allen et al., 2007; Karimi et al., 2013; Bastiaanssen et al., 2014; Javadian et al., 2019; Filippelli et al., 2022). However, ET only measures consumptive water use which is generally less than the amount of irrigation applied to the field.

The irrigation water requirement can be estimated through a soil water deficit model that assumes irrigation is only triggered when soil moisture is below a certain threshold and will be continued until the soil moisture reaches the field capacity (FC) or where the transpiration stress is removed (Chai et al., 2016). Bretreger et al., (2022), used a constellation of Landsat data to estimate crop growth stage and crop coefficient and later used this coefficient in a water deficit model to quantify the IWU. A conceptually similar approach was adopted by Sadri et al. (2022) to predict the soil water deficit (needed irrigation) with up to a 14-day lead time using several near-real-time satellite observations and precipitation prediction in a hybrid physical-statistical machine learning model (FarmCan). However, in practice, a farmer's decision to start or end the irrigation, does not necessarily follow the soil moisture status. For instance, a recent USDA survey in 2017 showed that 75% of farmers irrigated their fields based on a rule of thumb procedure, such as crop calendar, visual observations, and "what are neighbors doing!" (Zhang et al., 2021). Another study showed that the farmers that have experienced loss due to water shortages in the past are more likely to irrigate more frequently (Balasubramanya et al., 2022). Thus, it is quite common for an agricultural plot to be over-or under irrigated.

Soil moisture (SM) measurements are needed to account for over- or under-irrigation. Microwave (MW) remote sensing can measure soil moisture effectively under all weather conditions and is proven to carry irrigation signals (Lawston, Santanello, et al., 2017; Jalilvand et al., 2021). Brocca et al. (2018) and Jalilvand et al. (2019) have used satellite SM data with an SM-based inversion model (SM2RAIN model) to quantify irrigation water use. They relaxed some of the assumptions in the soil water deficit model to account for over-irrigation by allowing deep percolation to the lower soil layer and under-irrigation by adding a more sophisticated evapotranspiration module that allows

water-limited evapotranspiration. They quantify the irrigation water use based on the changes in the MW satellite soil moisture data from ASCAT and AMSR2. The results were consistent with in-situ observations over a large and intensely irrigated area, but failed over small agricultural practices, mainly due to spatial mismatch between coarse-scale MW products (> 25 km) and smallholder agricultural plots (<1km). Despite the promising results from SM2RAIN obtained from these studies, the SM data itself remains a major challenge to this model, in that a higher resolution SM product is needed to detect the irrigation signal (Jalilvand et al., 2019; Zaussinger et al., 2019; Dari et al., 2020; Foster et al., 2020; Massari et al., 2021; Modanesi et al., 2022), while, increasing the spatial resolution corresponds with narrower sensor swath width and less frequent retrievals (Das et al., 2019). Dari et al. (2020 and 2022) resolved the low temporal resolution issue by downscaling the coarse spatial but high temporal resolution data (e.g., SMAP Enhanced 9km product) using methods such as DiSPATCh. However, as the downscaled soil moisture product uses the thermal observations from MODIS platform that are affected by clouds and sense only the surface skin temperature, it might not capture the correct local SM dynamics in deeper than skin, which is one of the most important factor in the success of SM-based inverted water balance models such as the SM2RAIN. Therefore, the model might have a good mean performance at seasonal scale (e.g., due to compensatory effect of under-estimation during irrigation period and over-estimation during the non-irrigated period) but has difficulties in simulating the irrigation at shorter time steps.

Synergistic use of land surface model (LSM) and satellite data can address the issue of low frequency high-resolution SM observations. LSMs physically model land surface fluxes and state variables, including SM, by simultaneously solving the water and energy balance equations. LSMs may include an irrigation module to account for irrigation in the land surface processes (Ozdogan et al., 2010; Y. Pokhrel et al., 2012; Leng et al., 2014, 2017). However, the simplifying assumptions in the physics of the model and the errors in the input data can create large errors in the LSM simulation (Modanesi et al., 2021). In situ and satellite-based data assimilation (DA) can help reduce part of the random errors in the model simulation and correct the model state based on the observations. For example, Felfelani et al. (2018) assimilated SMAP SM observations (using a 1-D Kalman filter) to constrain the target SM in the Community Land Model (CLM) irrigation module and significantly reduced the irrigation water requirement error over an intensely irrigated area in the US. Modanesi et al., (2022) used an Ensemble Kalman Filter (EnKF) DA to directly assimilate Sentinel 1 backscatter in co- and cross-polarization into the Noah MP LSM with an irrigation scheme. They showed that assimilating Sentinel 1 backscatter in the VH polarization (that contains LAI information) can slightly improve irrigation simulations. Still, poor parametrization of the Noah-MP irrigation module does not allow the DA to improve the irrigation simulation significantly. Indeed, the irrigation module in most LSMs use a demand-driven formulation that works similar to the water deficit model and triggers irrigation when the root zone SM

(RZSM) drops below a certain threshold and continues irrigating until reaching a target RZSM (Haddeland et al., 2006; Lawston,; Sorooshian et al., 2011; Y. Pokhrel et al., 2012; Y. N. Pokhrel et al., 2016; Santanello Jr., et al., 2017; Felfelani et al., 2018). However, these models need information with a high level of uncertainty such as soil texture, crop type, and fractional irrigated area. Moreover, they do not explicitly account for the human choices in irrigation scheduling and amount.

Abolafia-Rosenzweig et al. (2019) shows that irrigation can be quantified using a Particle DA method such as a particle batch smoother (PBS). In this method, the LSM is forced with precipitation superimposed with a range of irrigation, then the satellite SM data is assimilated with an ensemble of model simulations (particles) in a defined length of time (window) and particles are weighted based on the proximity to all the SM observation in that window. These weights can then be traced to the forcing to obtain the best estimate of water input (irrigation + precipitation) and by subtracting precipitation the amount of irrigation can be calculated. The main advantage of the PBS over EnKF is that all model states are corrected in a physically consistent way rather than just updating one or two assimilated parameters and the weights from the analysis update can be used to update forcing as well. Moreover, as the SM is assimilated in a batch, even a 9-day interval between two satellite observations would lead to an R^2 larger than 85% relative to a known amount of irrigation (Abolafia-Rosenzweig et al., 2019).

In this study, we assimilate SMAP-Sentinel 1 (SMAP-S1) 1km SM data—that is proven to have the irrigation signal in both the first and second moments of SM time series (Jalilvand et al., 2021)—with the Variable Infiltration Capacity (VIC) model using a PBS DA approach. The main objectives of the study are:

1. Remove systematic biases between the LSM and the satellite observations prior to the data assimilation (Section 2.2)
2. Conduct a series of synthetic studies to evaluate the impact of system characteristics such as the frequency of the observations, knowledge of irrigation timing, and presence of noise in the observations on the irrigation estimation (Sections 2.3 and 4.1)
3. Quantify the irrigation water use over multiple irrigated and non-irrigated 1km pixels and evaluate the model performance against in-situ observed irrigation data (Sections 2.4 and 4.2)

The article is organized as follow: Section 2 describes the PBS method implementation (Section 2.1), the model calibration prior to the data assimilation (Section 2.2), the suite of synthetic experiments to evaluate the impact of different error sources on the DA system (Section 2.3), and the real-world experiments (Section 2.4). Section 3 introduces the study area (Section 3.1) and all the input data to the VIC LSM plus satellite SM data used for assimilation and in situ irrigation observations (Section 3.2). The results of the synthetic and real-world experiments are presented in Sections 4.1 and 4.2, respectively. Section

5 discusses the possible shortcomings and improvements in the PBS method by pointing to future satellite missions. Section 6 provides conclusions and the future prospective.

Methodology

A particle batch smoother (PBS) data assimilation approach is used to quantify the irrigation water use (IWU). Following Abolafia-Rosenzweig et al. (2019), we assimilate SMAP-S1 1km SM observations—that is proven to have irrigation signals (Jalilvand et al., 2021) over the study region—with VIC (version: 4.2d) LSM. We conduct a suite of synthetic experiments in an identical twin setup (Kumar et al., 2015; Abolafia-Rosenzweig et al., 2019), where truth SM is created by forcing VIC with precipitation plus a known amount of irrigation, and then evaluate the model performance under different system characteristics such as known or unknown irrigation timing, different frequency of observation, and various noise levels. For optimum DA performance, the systematic bias between the model and observations must be addressed (Kumar et al., 2012). We choose an *a priori* bias correction strategy by calibrating the model against observations (as opposed to scaling the observations to the model climatology). Finally, SMAP-S1 SM data are assimilated over multiple irrigated and non-irrigated pixels and simulated irrigation using the PBS method is evaluated against in-situ irrigation observations.

Particle Batch Smoother

We use a particle batch smoother (PBS) algorithm to assimilate SMAP-S1 SM observations with the VIC LSM. PBS is a non-sequential extension of a particle filter (PF) in which a series of observations within a window of time is assimilated in a batch to correct the model state. It is shown that using the same observation data, PBS yields better results compared to the PF (Dong et al., 2015). The main distinctions of PBS compared to the widely used ensemble Kalman Smoother (EnKS) is that: 1) the model simulation weight can be traced to the corresponding input forcing (here, precipitation plus irrigation) to form the posterior probability distribution function (PDF) of the forcing, and 2) PBS maintains mass & energy balance of ensemble members.

Here we describe the PBS implementation. Readers are referred to (Abolafia-Rosenzweig et al., 2019; Dong et al., 2015) for the detailed presentation of the method.

The precipitation forcing is created by superimposing a random irrigation value during the irrigation season.

$$P^{i}_{\text{particle}} = P_{\text{obs}} + IRRG^{i}(r) \quad (1)$$

Where P^i_{particle} shows the precipitation forcing for each particle, IRR$G^i(r)$ is a random sample from a uniform distribution of irrigation. Since here we choose to have 99 particles, P_{particle} would be a 99×1 vector. The range of irrigation (r) is chosen to be between 0 to 12 mm /day during the irrigation season (May-August inclusive) and zero elsewhere. We use two scenarios for adding the irrigation: 1) we assumed that we know the irrigation timing or, 2) the irrigation timing is unknown, and the irrigation is applied continuously. An ensemble of model states evolves in parallel using a forward model.

$$x^i_t = f\left(x^i_{t-1}, u^i_t, b^i\right) + w^i_t \quad (2)$$

Where x^i_t is the model state for particle i at time step t, u^i_t is the forcing dataset, b^i is a vector of time-invariant model parameters, w^i_t is the model error, which is assumed to be normally distributed and, f is the forward model (VIC 4.2d).

The likelihood of observed, y, given particle estimate of, x, is calculated based on all observations within the window of length L.

$$p\left(y_{t-L+1:t} \mid x^i_{t-L+1:t}\right) = \prod_{j=t-L+1}^{t} \frac{1}{(2\pi)^{\frac{n}{2}} \times \det(C_v)^{(\frac{1}{2})}} e^{-0.5\left(y_j - x^i_j\right)^T C_V^{-1}\left(y_j - x^i_j\right)} \quad (3)$$

Where $t - L + 1 : t$ represents the window, n represents the number of states or the fluxes that are assimilated (here only SM is assimilated thus, $n = 1$), C_v is the observation error covariance. We used the SMAP-S1 prescribed error for C_v. When the window length is $L = 1$ then the observations are assimilated sequentially otherwise they are assimilated in a single batch in each window. The weight for each particle (w^i_t) in each window is calculated by normalizing the likelihood of each particle:

$$w^i_t = \frac{p(y_{t-L+1:t} \mid x^i_{t-L+1:t})}{\sum_{i=1}^{N} p(y_{t-L+1:t} \mid x^i_{t-L+1:t})} \quad (4)$$

It is recommended to resample the weights at the beginning of each window to avoid weight degeneration (a situation where a negligible weight is assigned to most of the particles) (Moradkhani et al., 2005). We used sequential weights resampling to resample particles based on the weights in the previous window (Gordon et al., 1993; Weerts & el Serafy, 2006). This method gives particles with higher weights a greater chance of propagating their state into the next window as an initial condition (Dong et al., 2015).

Finally, the expected time series of precipitation plus irrigation ($A_{PBS,t}$) will be

$$A_{PBS,t} = \sum_{i=1}^{N} w_t^i \; P^i_{particle,t} \quad (3)$$

Where N is the number of particles (here $N = 99$) and $P^i_{particle,t}$ is the particle i forcing at time t. The best-simulated irrigation time series is estimated by subtracting observed precipitation (P_{obs}) from the $A_{PBS,t}$.

A Priori bias correction

Systematic biases between the model and the satellite observations (from SMAP-S1) must be addressed prior to the analysis step within data assimilation. We acknowledge that both the SMAP-S1 and the model SM values are different indices of soil wetness, but here we assume that SMAP-S1 has observability relative to the in situ measurements. To remove biases, either observations are scaled to conform to the model's climatology (e.g., through CDF matching), or the model is calibrated against observation climatology. The key consideration is that the bias correction approach should preserve observed irrigation signals while removing biases between simulated and observed SM (excluding biases imposed by unmodeled irrigation). The problem with rescaling methods such as CDF-matching (REF) is that it might remove unmodeled human-induced signals in SM observations, such as irrigation (Kumar et al., 2015). Therefore, we use the model calibration approach in a batch mode, as suggested by Kumar et al. (2012), where a set of observations are used to estimate the model parameters by minimizing the difference between the model and observations. We choose to only calibrate the model during the rainy season to avoid erasing the unmodeled irrigation process. The objective function for model calibration is minimizing the absolute mean bias between the modeled and the observed SMAP-S1 SM during the rainy season. According to the sensitivity analysis carried out by Zhou et al. (2020), the two main parameters that strongly change the first and second moment of the simulated SM are BLKDN (bulk density) and EXPT (the exponent in the Campbell's equation for soil hydraulic properties (Campbell, 1974)). We choose to fit the BLKDN (variation range from 1200 to 1400 [kg/m^3]) and EXPT (variation range from 3 to 20 [-]) for SM model calibration. The ranges are chosen based on the soil physical properties of the case study obtained from SoilGrid 250 m (www.openlandmap.org) data (Hengl et al., 2017).

Synthetic experiment sensitivity analysis

We use a suite of synthetic experiments to evaluate the sensitivity of the DA model to the different error sources. The model was evaluated by introducing sources of error sequentially and combined as shown in Table 1. The synthetic truth was created by forcing the VIC model with a known amount of irrigation plus precipitation. Synthetic observations were generated by sampling the truth simulation at daily, SMAP-S1 frequency, and every 12 days (SMAP-Sentinel 1 A only). To evaluate the impact of noise in the satellite retrievals we run ex-

periments by imposing random 0-mean Gaussian noise to the synthetic SM retrievals with a standard error of 0.05 m^3/m^3 (unbiased root mean square error (ubRMSE) of SMAP-S1, as mentioned in Das et al., 2019). We run each of these experiments (EXP No 7-12 in Table 1), 20 times (20 data assimilation experiments with unique sets of random noise imposed on synthetic observations) and report the mean irrigation of 20 realizations as the final simulated irrigation of that experiment. We further seek to evaluate DA performance when irrigation timing is known or unknown. In the case of unknown irrigation, we applied irrigation continuously (all day, every day) throughout the irrigation season (May-August inclusive). As the range of plausible irrigation applications is varying based on the climate, crop type, and human choices, we evaluate the sensitivity of DA performance to changing the range of superimposed irrigation during the irrigation season.

Real world experiment

We perform real-world data assimilation experiments over multiple irrigated (IR) and non-irrigated (nIR) pixels in our study region. According to our previous study (Jalilvand et al., 2021) a high mean absolute deviation (MAD) in the SMAP-S1 SM time series during the irrigation season is an indicator of irrigation signal being captured by the satellite observations. Therefore, 4 irrigated pixels with a high MAD value that are covering an irrigation channel (for which in situ irrigation data is available) are selected as the IR pixels. Simulated irrigation depth is divided by the fraction of irrigated area in each pixel that is obtained from the landuse map of the region (Mousivand et al., 2020). We run the model over nIR pixels to estimate the amount of false irrigation over the non-irrigated area. Thereby, 7 nIR pixels located nearby the irrigated area (within 36 km SMAP radiometer footprint that also covers irrigated pixels) all with low MAD value and landuse/landcover type of range land or rainfed agricultural are chosen as the nIR pixels (nIR 01). To test the impact of possible irrigation signal leakage from the IR pixels to the neighboring nIR pixels we choose to run the model over 4 other nIR pixels that are located far away from the irrigated pixels (outside of the 36 km base SMAP radiometer footprint that covers the irrigated area) (nIR 02). All the location of the pixel, underlying MAD value, and the location of irrigated channels are shown in Figure 1.

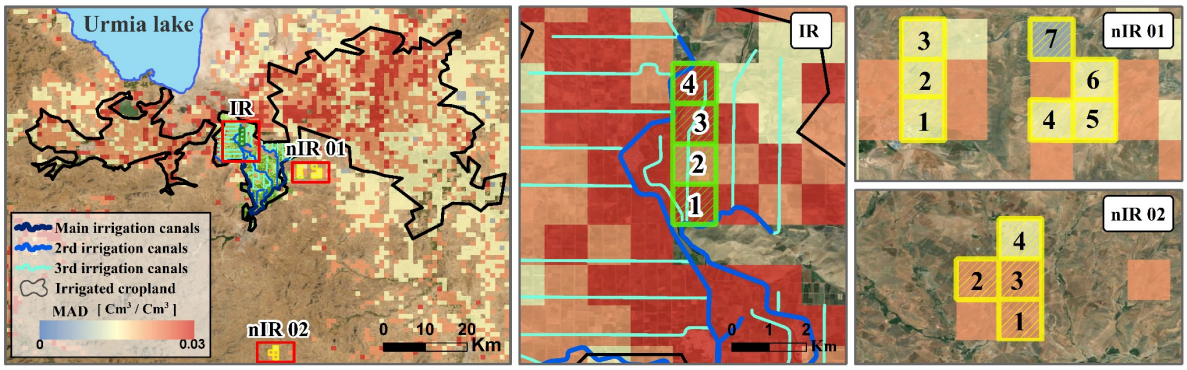

Figure 1 Overview of the study area. Irrigated (IR) and the non-irrigated (nIR) pixels are chosen based on the SM MAD value (higher MAD for the IR and lower MAD for the nIR) according to a) location of the irrigated cropland area b) irrigated pixels (IR) covering one of the irrigated channels for which in situ data is available c) non-irrigated pixels within the 36km of irrigated pixels (nIR 01) d) non-irrigated pixels (nIR 02) farther down the irrigated area (outside of the 36 km base SMAP radiometer footprint that covers the irrigated area)

The LSM (VIC) simulation forced with the precipitation only is termed the open-loop (OL) run, the VIC simulation calibrated against SMAP-S1 SM observations and forced with precipitation is used as the calibrated simulation (CAL). The weighted average of simulations forced with precipitation plus a random amount of irrigation used as the particles is termed the PBS. PBS simulations are compared with the observed irrigation (Section 3.2.2). Simulated irrigation over the irrigated and non-irrigated pixels are tested for the difference of medians using the Wilcoxon right-tale rank-sum test.

Data and the study area

Study area

Urmia lake has experienced a rapid decline of water volume in the past two decades due to anthropogenic activities and climate change. On the human part, most of the drying is blamed on the expansion of irrigated agriculture around all the tributaries to the lake (AghaKouchak et al., 2015; Parsinejad et al., 2022). Indeed, the agricultural water demand is more than all the surface water input to the lake combined (Schulz et al., 2020). To stop the drying of the lake different measures have been taken by the Urmia Lake Restoration Program (ULRP) including a 40% reduction in irrigation water use that specifically targeted the agricultural sector (Sima et al., 2021). Later studies show that a 10% more reduction is needed to buffer the impact of climate change (Schulz et al., 2020). 60% of lake Urmia's surface water is coming from four southern rivers (Zarineh rood, Simineh Rood, Mahabad, and Gadarchay) that pass through three major

irrigated agricultural regions (Miandoab, Mahabad, and Naghadeh). Mahabad has a fully established irrigation network downstream of the Mahabad Dam and gravity irrigation is the common irrigation practice in the region (Shadkam et al., 2016). The main crops cultivated in Mahabad are wheat, barley, and alfalfa, which are usually irrigated between May to the end of August (Zaman et al., 2016).

Data

VIC model

Variable Infiltration Capacity (VIC) is a distributed hydrological model (Liang et al., 1994) that simultaneously solves the water and energy balance equation on each grid cell independently. We choose to work with VIC 4.2d version that has the ability to simulate partial vegetation cover and photosynthesis and can input time-varying vegetation parameters. We run the model at EASE-GRID 2.0, 1 km^2 grid (Brodzik et al., 2012) and hourly time steps. Three soil layers are considered in the model implementation with 0.1 m, 0.9 m, and 1.976 m depth from the top to the bottom. The first soil layer depth is chosen to be equal to SMAP nominal sensing depth (10 cm) which according to the recent study by Feldman et al. (2022) proved to be deeper than 5 cm.

The atmospheric forcing inputs are hourly precipitation, minimum and maximum temperature, and wind speed. The vegetation forcing including vegetation fraction, Leaf Area index (LAI), and Albedo, and the soil parameter file are created based on the 5 km soil data from soil grid 250 m (Hengl et al., 2017).

Atmospheric Forcing

Daily Integrated Multi-satellitE Retrievals for GPM (IMERG) final run V06 product (Huffman et al., 2019) at 0.1° resolution is used as the precipitation forcing. Wind speed and maximum and minimum air temperature data are obtained from the GLDAS Noah Land Surface Model L4 3-hourly 0.25° V2.1 (GLDAS_NOAH025_3H) (Rodell et al., 2004). Following Abolafia-Rosenzweig et al. (2019), the wind and the precipitation datasets are bicubically resampled while the temperature dataset is disaggregated bilinearly to the EASE-GRID 2.0, 1 km^2 grid. Hourly disaggregation of daily precipitation is performed by equally dividing the daily precipitation throughout the 24 hours and the hourly wind and air temperature are created by replicating the same value for each 3-hour interval. We acknowledge that downscaling wind and temperature data is an error prone process and can play a role in simulated errors at the 1km resolution, but to the authors' knowledge, the GLDAS data was the best option available in this region. Furthermore, our case study is located in an area of low topographic complexity which tends to have lesser spatial heterogeneity in temperature and wind. We use the finer resolution product (IMERG) for precipitation—which is the primary driver of SM variations—to reduce these errors.

Vegetation Forcing

Vegetation forcing variables—LAI, Albedo, and vegetation fraction—are from MODIS products. 8-Day, 500 m MODIS combined Leaf Area Index (MCD15A2H, V006) is used for the LAI forcing, daily 500 m MODIS combined Albedo (MCD43A3, V006) is used for the Albedo forcing, and 16-Day, 500 m EVI (MYD13A1, V006) is used to calculate the vegetation fraction.

Soil Parameters

VIC Soil parameters are generated from the 250 m SoilGrid data (Hengl et al., 2017) using soil empirical equations (Saxton & Rawls, 2006) at 5 km^2 spatial resolution. This data is upscaled to the model grid using the drop-in-the-bucket aggregation approach.

SMAP-Sentinel 1

We use an updated version of SMAP-S1 1km SM (Das et al., 2019; Das et al., 2020) with dynamic vegetation water content that proves to have the irrigation signal in both the first and second moment of the SM time series (Jalilvand et al., 2021). The Sentinel 1A AM pass is exclusively merged with either the same day morning or the previous day afternoon SMAP crossing to ensure the stability of SM content between two successive radiometer and radar retrievals. The data is further filtered on pixel level based on time differences between the Sentinel 1A and SMAP retrievals.

In situ irrigation data

Since 2020, ULRP has installed multiple flowmeters on a number of third-order channel in the Mahabad irrigation network. Each of the flowmeters measures the water allotment of roughly 3 km^2 of the irrigation cropland. The volume of the water, the area that is irrigated, and the start and the end of each irrigation event are recorded. The depth of irrigation (mm/hour) at each irrigation event is obtained by dividing the volumetric irrigation by the area irrigated and number of irrigation hours.

Result

Synthetic experiment

The results from the synthetic experiments (summarized in Table 1) show that prior knowledge of irrigation timing has a significant impact on the accuracy of estimated irrigation, and assuming continuous irrigation tends to cause overestimates. Indeed, in most of the simulations with known irrigation timing, we obtain a bias of less than 1%, while when the irrigation schedule is unknown, the average bias between simulated and observed irrigation increases to 22% and RMSE increases by 5-10 times. Moreover, when irrigation timing is unknown,

the model fails to capture the temporal pattern of irrigation (R^2 at hourly time-series drop to less than 40%). Imposing noise on synthetic observations resulted in less accurate irrigation; although, more frequent observations can help reduce the noise impact as they provide more irrigation signal rather than noise (Abolafia-Rosenzweig et al., 2019). The uncertainty in synthetic observations is shown by the red band in the irrigation plots in Figure 2 which are anticorrelated to the frequency of the observations in each window. This means the possible range of estimated irrigation can significantly increase (model uncertainty increases) when the temporal resolution of the observations, for example, satellite SM, is low. This error can also propagate to the next window as potentially inaccurate particles with high weights have a high probability of propagating to the next window in the resampling process.

In the zero-noise experiments, the bias is persistently positive (irrigation is overestimated) in both known or unknown irrigation timing scenarios, whereas; when random noise is imposed and irrigation timing is known (EXP No 7, 9 and 11) the bias is nearly zero or negative (irrigation is underestimated). This is likely partially attributable to missing some irrigation events due to lower observation frequency.

Table 1- summary of the synthetic experiment results

@ >p(- 12) * >p(- 12) * >p(- 12) * >p(- 12) * >p(- 12) * >p(- 12) * >p(- 12) * @ Exp No & Noise & Observation frequency & Irrigation timing & Accumulated irrigation Bias (%) & Irrigation RMSE (mm/hr) & Irrigation R^2 &

No noise

& Daily & known & +0.51 & 0.014 & 0.993
2 & & & continuous & +16.67 & 0.141 & 0.394
3 & & SMAP-S1/NISAR frequency & known & +0.41 & 0.026 & 0.977
4 & & & continuous & +22.93 & 0.143 & 0.394
5 & & 12 days

(Sentinel 1A-only) & known & +0.712 & 0.029 & 0.9735
6 & & & continuous & +26.42 & 0.154 & 0.318
7 &

With Noise

20 realization mean

& Daily & known & +0.09 & 0.017 & 0.990
8 & & & continuous & +18.25 & 0.143 & 0.381
9 & & SMAP-S1/NISAR

frequency & known & -3.05 & 0.043 & 0.943
10 & & & continuous & +24.93 & 0.150 & 0.341
11 & & 12 days

(Sentinel 1A-only) & known & -7.43 & 0.043 & 0.953
12 & & & continuous & +25.71 & 0.161 & 0.254

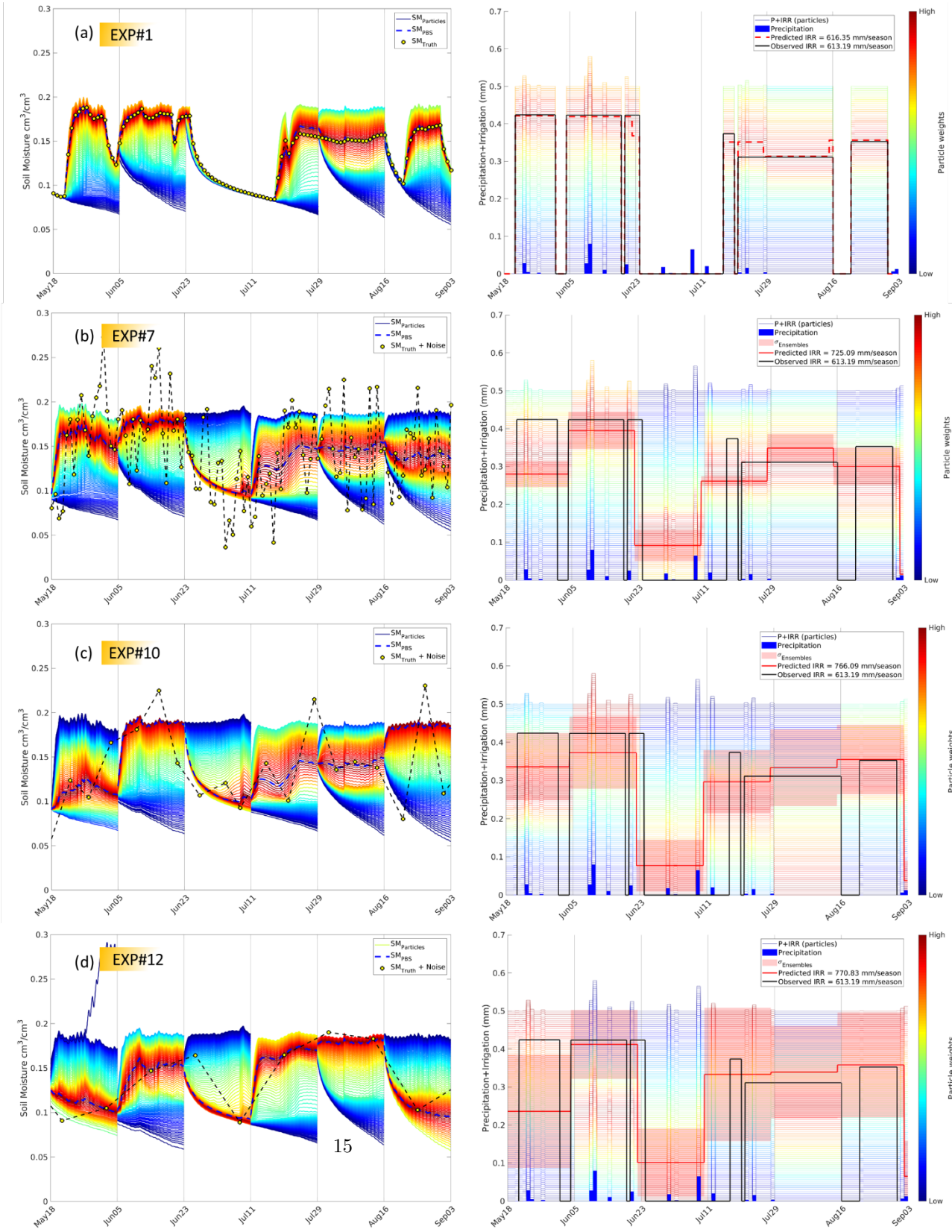
(a) EXP#1
(b) EXP#7
(c) EXP#10
(d) EXP#12
Soil Moisture cm³/cm³
Precipitation+Irrigation (mm)
SM_Particles
SM_PBS
SM_Truth
SM_Truth + Noise
P+IRR (particles)
Precipitation
σ_Ensembles
Predicted IRR = 616.35 mm/season
Predicted IRR = 725.09 mm/season
Predicted IRR = 766.09 mm/season
Predicted IRR = 770.83 mm/season
Observed IRR = 613.19 mm/season
Particle weights
High
Low
May18
Jun05
Jun23
Jul11
Jul29
Aug16
Sep03

Figure 2 Synthetic experiment shows that knowing irrigation timing and having more frequent SM retrievals significantly improves simulated irrigation. The left-side plots show the particles ($\mathbf{SM}_{\text{particles}}$) for one model realization that are colored based on closeness to the synthetic truth SM ($\mathbf{SM}_{\text{truth}}$) shown as a dashed black line and yellow circles, and the dashed blue line shows the weighted average of all particles ($\mathbf{SM}_{\text{PBS}}$). The right-side plots show the corresponding irrigation time series where the best irrigation simulation is shown as the dashed red line (average of 10 realizations when random noise is added) and observed irrigation is the solid black line, the light red band showing one standard deviation of 10 simulations with random noise. Synthetic experiments are conducted with different assumptions: (a) EXP No 1: ideal situation; synthetic truth at daily timesteps, without adding noise and knowing the irrigation timing, (b) EXP No 7: synthetic truth at daily timestep with random noise added and not knowing the irrigation timing, (c) EXP No 10: synthetic truth resampled at the SMAP-S1 frequency, with random noise added and not knowing the irrigation timing and, (d) EXP No 12: synthetic truth resampled at the SMAP-Sentinel 1 A only frequency (every 12 days), with random noise added and not knowing the irrigation timing.

Real-world experiment

The model underestimates seasonal cumulative irrigation at the irrigated pixels by -18.6% (average of 4 IR pixels) when irrigation timing is known and overestimates irrigation by 5.5% when the irrigation timing is unknown (Figure 3). The underestimation in the known irrigation simulation is higher for the real-world experiment than in the corresponding synthetic experiment (Table 1). This might be due to losing part of the irrigation signal in the SMAP-S1A SM retrievals because of 7-day overpass interval. The coarse spatial resolution of SMAP-S1 1km observations relative to plot scale agriculture, imperfect LSM physics, and uncertainty in LSM input data are among the factors contributing to the prediction errors. On the other hand, mean irrigation efficiency for the entire Urmia Lake basin is less than 40% (Shadkam et al., 2016). Mahabad plain though, has an established lined irrigation network and might have a higher efficiency; however, a portion of water is inevitably lost in the delivery system after the measuring station. Moreover, there are reports of illegal surface water extraction from the irrigation channels in the region. Thus, in practice, the amount of water that is used for irrigation is lower and can explain a part of underestimation by PBS.

Simulations using unknown irrigation timing result in more accurate accumulated irrigation relative to the corresponding synthetic experiment, but this is attributable to compensatory errors (i.e., the right answer for the wrong reason). In the continuous simulation, we still mostly underestimate irrigation during the irrigation season (especially from June to the end of the irrigation season), but the estimation of some irrigation amount during the gap in the irrigation application compensates for underestimation in the irrigation period.

The magenta and the green dashed line in the SM plots of Figure 3 (a and c) show the OL and CAL runs that demonstrate how model calibration removes the systematic bias at the beginning of the simulation and how PBS DA introduce the unmodeled irrigation process and improves the simulated SM relative to SMAP-S1 observations.

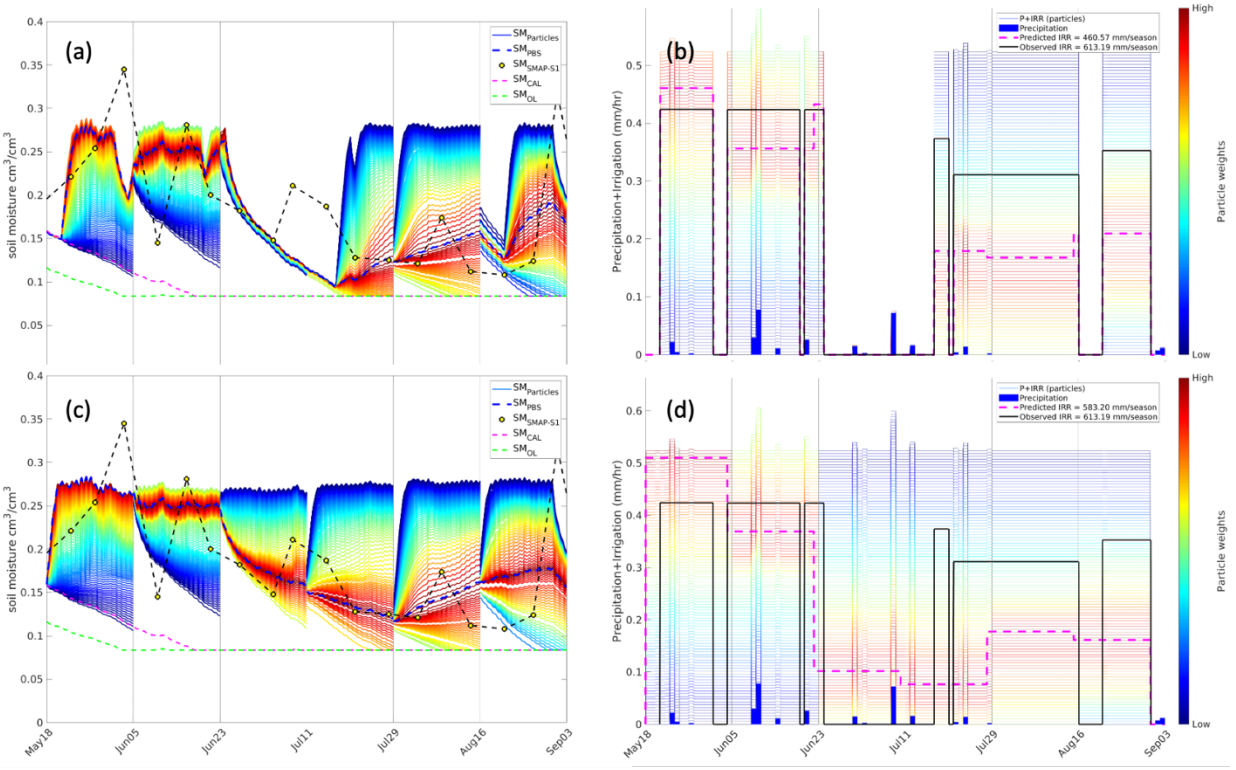

Figure 3 Assimilating SMAP-S1 SM data using a PBS approach over irrigated pixels leads to an underestimation of irrigation. (a) SM timeseries of 99 particles colored by the weights assigned based on the proximity to SMAP-S1A SM observations (dashed-black line and yellow dots) and the best-simulated SM (dashed blue line) when irrigation timing is known, and (c) when it is unknown. The dashed magenta and green line in the SM time series shows the calibrated and OL runs. (b) The corresponding time series of IRR particles constructed by tracing the weights to the particle forcing and the best estimate of irrigation (dashed magenta line) when irrigation timing is known and (d) when it is unknown.

We estimate nearly zero irrigation in non-irrigated pixels (Figure 4) far away from the irrigated pixels (outside of the 36 km radiometer base SMAP product footprint covering the irrigated area). The estimated irrigation in the nIR pixels that are located within the same base radiometer SMAP product as the irrigated pixels is significantly higher than the nIR pixels far away from the IR

pixels, which can be due to the possible leakage of the irrigation signal from the IR pixels to the nearby nIR pixels and indicate room for improvement in the downscaling approach. Yet the amount of irrigation at these neighboring nIR pixels (nIR01) is significantly lower than the IR pixels (Figure 5).

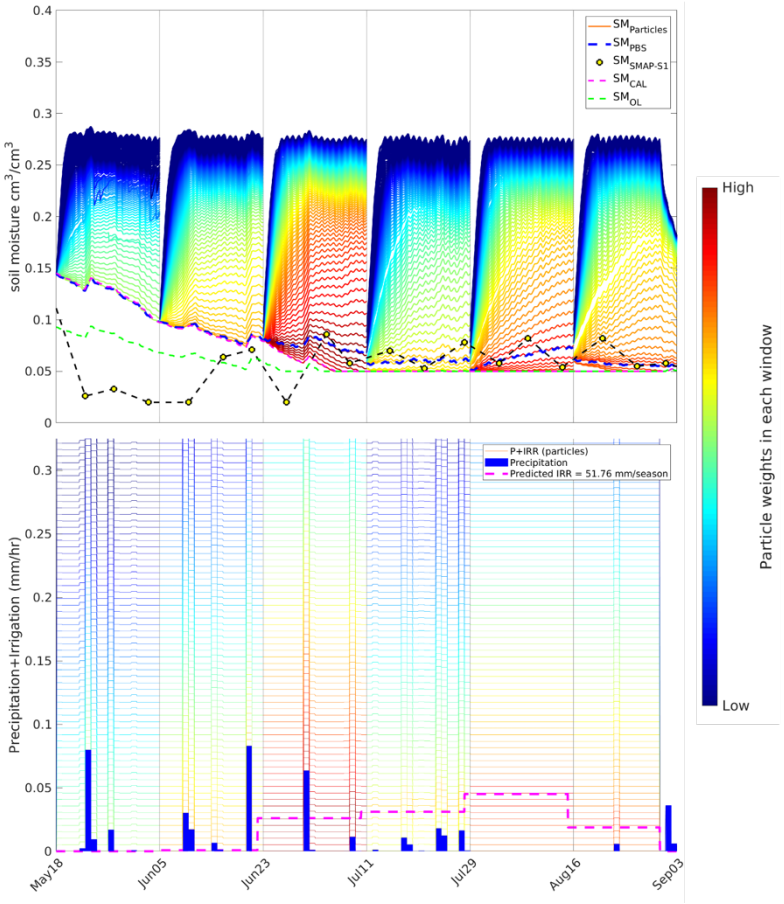

Figure 4 Nearly zero irrigation is estimated over a non-irrigated pixel far away from the irrigated area. (a) SM time series of 99 particles colored by the weights derived from the proximity to the SMAP-S1A SM data (black dashed-(yellow) dotted line) and the best estimate of SM (dashed blue line) over a non-irrigated pixel. The dashed-magenta and green line in (a) show the CAL and OL run, respectively. (b) The corresponding time series of IRR constructed by tracing the weights to the particle forcing and the best estimate of irrigation (dashed magenta line).

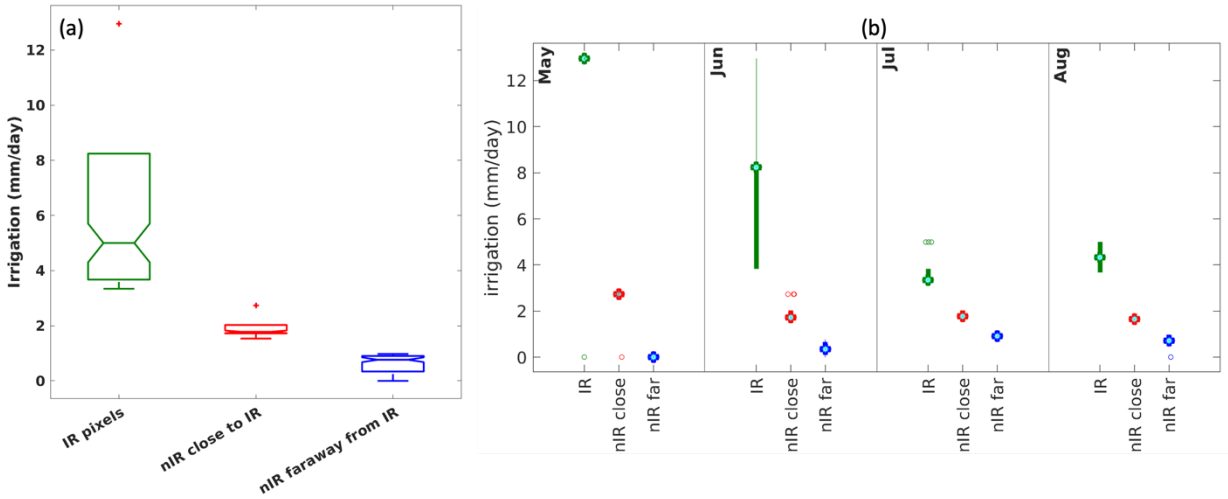

Figure 5 Significantly higher irrigation is obtained over the IR pixels (green) compared to nIR pixels close to the irrigated area (red) and nIR pixels far away from the irrigated area (blue), (a) during the irrigation season and, (b) during each month of the irrigation season.

Calibration theoretically remove systematic biases between LSM and observed SM, excluding differences caused by unmodeled processes such as irrigation. Figure 6 shows that calibration alone improves simulated SM RMSE relative to SMAP-S1 SM observations over the irrigated pixels (by nearly 10% on average) compared to the OL run during the irrigation season. The PBS DA accounts for the remaining 50% improvement in RMSE by introducing the unmodeled irrigation forcing and contributing to the reduction of random noise.

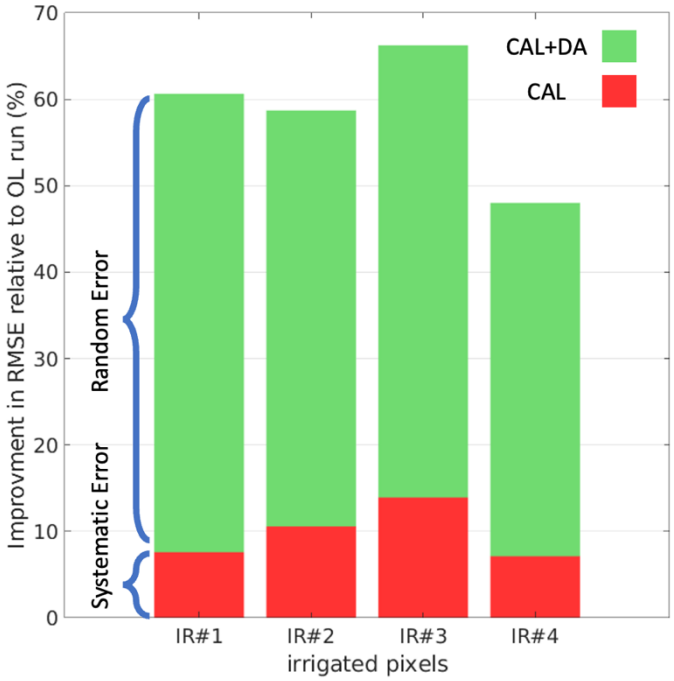

Figure 6 Improvement in SM RMSE against SMAP-S1 observations relative to OL run after model calibration (red bar) and after both calibration and data assimilation (red and green bar) during the irrigation season

Discussion

The impact of less frequent retrieval on the estimated irrigation

The impact of less frequent SM retrievals on the SM estimation is two-fold: 1) it is most likely that an irrigation event is missed especially over the arid and semi-arid areas where the SM memory is low (McColl, Alemohammad, et al., 2017; McColl, Wang, et al., 2017). This favors significant underestimation of irrigation. 2) Having multiple retrievals in one smoothing window can average out an outlier observation, however having an outlier (e.g., a very noisy observation) in a sparse SM time series at either end of the SM spectrum (saturated or residual SM) can lead to choosing the wettest or the driest particle in that window and consecutively over-or underestimation of the irrigation, respectively.

Possible problems with an unknown superimposed irrigation range

The maximum superimposed irrigation value can be among the unknowns in many regions. When SM observations are close to saturation, the PBS model will favor the wettest particles. Therefore, if 10 mm irrigation results in the soil saturation in one window, choosing a 40 mm/day as the maximum of the supplement irrigation can result in a 4 times higher irrigation estimation in that window as SM cannot increase beyond saturation. A similar situation can be seen in the first window of Figure 3, where a saturated observation resulted in the selection of the wettest particle and the overestimation of irrigation in that window. Hence, this methodology is not appropriate for irrigation quantification over regions that maintain saturated soils via irrigation.

Posterior bias correction

The false irrigation estimate at non-irrigated pixels can be treated as the model's positive bias and be removed from the irrigation estimation over the irrigated pixels. However, irrigation should be the only difference between the IR and the nIR pixels, otherwise the posterior bias correction might remove the true irrigation signal. Jalilvand et al. (2019) argued that choosing an adjacent nIR pixel for the posterior bias correction can maximize the climate similarity as the estimated irrigation at the nIR pixel may exclusively cause by the model bias rather than a different precipitation pattern. Brombacher et al. (2022) used a hydrological similarity concept (van Eekelen et al., 2015) to compare actual evapotranspiration (ET_{act}) of an IR pixel with an average ET_{act} of natural (nIR) pixels to calculate the ET_{act} caused by the irrigation (incremental ET). They define hydrological similarity based on a set of features derived from soil texture, DEM, reference ET, and precipitation datasets. The same concept can be adopted in future studies for the posterior bias correction of irrigation estimated by the PBS method.

Moving forward and future consideration

Upcoming high-resolution satellite missions

Future satellite missions such as the NASA-ISRO SAR mission (NISAR) with 200 m spatial resolution (Figure 7) and retrieval frequency of 6 days can significantly improve the irrigation simulation and quantification as it can observe SM changes at the scale relevant to the most smallholder plots globally. Indeed, the non-irrigated area within the 1 km^2 SMAP-S1 pixel can contribute to the SM retrieval and alleviate the irrigation signal. This fact is confirmed by estimating significantly higher irrigation in the synthetic experiment (where it is assumed that the satellite SM product backs out the entire irrigation signal), compared to the corresponding real-world experiment.

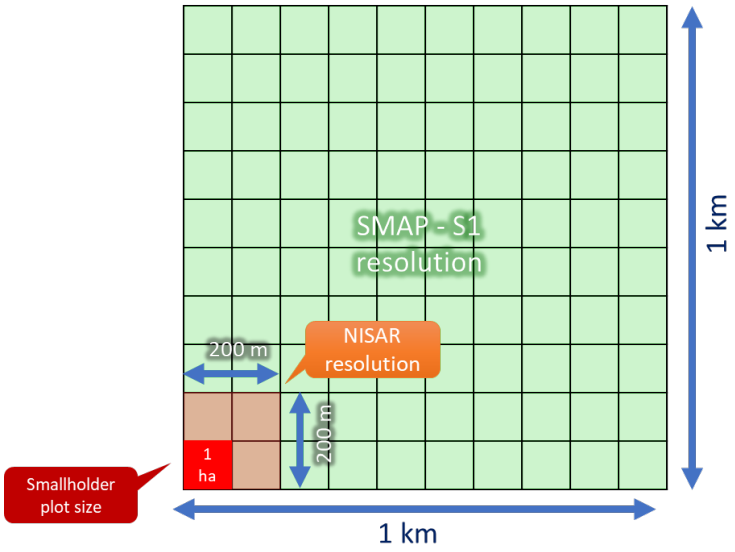

Figure 7 The future NISAR high-resolution SM data can significantly improve the irrigation simulation at the plot scale using the PBS approach.

Smart particles

Particles can be designed to not superimpose irrigation unless an irrigation event in an irrigated pixel is detected by the satellite. In our previous study (Jalilvand et al., 2021), we demonstrate that the IR pixels show a significantly higher variation (MAD value) in the SM during the irrigation season compared to the nIR pixels. Thus, the satellite SM MAD value can be used to filter non-irrigated pixels prior to the DA. Furthermore, irrigation can be added to the precipitation forcing of the IR pixels when a positive increment in the SM, which is not caused by precipitation, is observed. This is especially applicable when more frequent observations, for example, daily, are available from high-resolution (<1km) satellite SM data.

Conclusion

Irrigation is the largest human-engineered modification in the global water budget that is largely unknown and poorly represented in the land surface and hydrological models. Irrigation can directly change the SM which can be detected through microwave (MW) remote sensing. In this study, we used a particle batch smoother (PBS) approach to assimilate the SMAP-S1 1km SM data with the VIC (4.2d) land surface model to quantify the irrigation water use. The main findings are:

1. By calibrating the model against SMAP-S1 observations during the rainy

season we reduced systematic biases between the LSM and satellite observed SM. Unlike commonly used rescaling approaches such as CDF-matching, this bias correction strategy allows for preserving and incorporating observed irrigation signals through data assimilation.

2. We evaluate the impact of known error sources by conducting a suite of synthetic experiments. Results showed that the knowledge of the irrigation timing can significantly improve the irrigation simulation. Moreover, the frequency of observations can help reduce the impact of random noise in the observations.

3. The method is applied to multiple irrigated pixels for which in-situ irrigation data was available. We underestimate the irrigation by an average of 18.6% which can be due to losing part of the irrigation signal in the SMAP-S1 1km SM retrievals. The presence of non-irrigated areas in 1km SMAP-S1 SM data can also alleviate the irrigation signal from smallholder plots.

4. We obtain significantly lower irrigation over the non-irrigated pixels compared to the irrigated pixels. The false irrigation estimated at the nIR pixels within the same SMAP 36km base pixel as the IR pixels, was significantly higher than the far away nIR pixels outside of the 36km SMAP base footprint. This may be evidence of irrigation signal leakage from irrigated pixels to nearby non-irrigated pixels.

5. Calibration of the model resulted in an average 10% improvement in the RMSE while assimilation of SMAP-S1 SM and superimposing the unmodeled irrigation forcing with the PBS approach was responsible for an additional 50% improvement in the RMSE over the irrigated pixels during the irrigation season.

6. If the farmers provide their irrigation schedule (i.e., start and end of each irrigation event), we can theoretically quantify the amount of seasonal irrigation with 3% accuracy and ~95% correlation (Table 1, EXP No. 9) using a weekly remotely sensed SM product that maintains the majority of irrigation signals (potentially NISAR 200m SM data).

7. Improved High-resolution and accurate observations possibly through the future satellite missions (e.g., NISAR) would reduce the impact of leakage errors and can help to circumvent the issue of unknown irrigation schedules

References

Abolafia-Rosenzweig, R., Livneh, B., Small, E. E., & Kumar, S. V. (2019). Soil moisture Data Assimilation to Estimate Irrigation Water Use. *Journal of Advances in Modeling Earth Systems*, *11*(11), 3670–3690. https://doi.org/10.1029/2019MS001797

Abbott, B. W., Bishop, K., Zarnetske, J. P., Minaudo, C., Chapin, F. S., Krause, S., Hannah, D. M., Conner, L., Ellison, D., Godsey, S. E., Plont, S., Marçais, J., Kolbe, T., Huebner, A., Frei, R. J., Hampton, T., Gu, S., Buhman, M., Sara Sayedi, S., … Pinay, G. (2019). Human domination of the global water cycle absent from depictions and perceptions. *Nature Geoscience*, *12*(7), 533–540. https://doi.org/10.1038/s41561-019-0374-y

AghaKouchak, A., Norouzi, H., Madani, K., Mirchi, A., Azarderakhsh, M., Nazemi, A., Nasrollahi, N., Farahmand, A., Mehran, A., & Hasanzadeh, E. (2015). Aral Sea syndrome desiccates Lake Urmia: Call for action. *Journal of Great Lakes Research*, *41*(1), 307–311. https://doi.org/10.1016/j.jglr.2014.12.007

al Naber, M., & Molle, F. (2017). Controlling groundwater over abstraction: state policies vs local practices in the Jordan highlands. *Water Policy*, *19*(4), 692–708. https://doi.org/10.2166/wp.2017.127

Allen, R. G., Pereira, L. S., Smith, M., Raes, D., & Wright, J. L. (2005). FAO-56 Dual Crop Coefficient Method for Estimating Evaporation from Soil and Application Extensions. *Journal of Irrigation and Drainage Engineering*, *131*(1), 2–13. https://doi.org/10.1061/(ASCE)0733-9437(2005)131:1(2)

Allen, R. G., Tasumi, M., & Trezza, R. (2007). Satellite-Based Energy Balance for Mapping Evapotranspiration with Internalized Calibration (METRIC)—Model. *Journal of Irrigation and Drainage Engineering*, *133*(4), 380–394. https://doi.org/10.1061/(ASCE)0733-9437(2007)133:4(380)

Balasubramanya, S., & Stifel, D. (2020). Viewpoint: Water, agriculture & poverty in an era of climate change: Why do we know so little? *Food Policy*, *93*, 101905. https://doi.org/10.1016/j.foodpol.2020.101905

Balasubramanya, S., Stifel, D., & McDonnell, R. (2022). Water shortages, irrigation frequency, and preference for technologies and agricultural services: The case of Jordan*. *Irrigation and Drainage*, *71*(2), 437–451. https://doi.org/10.1002/ird.2650

Bastiaanssen, W., Karimi, P., Rebelo, L.-M., Duan, Z., Senay, G., Muthuwatte, L., & Smakhtin, V. (2014). Earth Observation Based Assessment of the Water Production and Water Consumption of Nile Basin Agro-Ecosystems. *Remote Sensing*, *6*(11), 10306–10334. https://doi.org/10.3390/rs61110306

Bretreger, D., Yeo, I.-Y., & Hancock, G. (2022). Quantifying irrigation water use with remote sensing: Soil water deficit modelling with uncertain soil parameters. *Agricultural Water Management*, *260*, 107299. https://doi.org/10.1016/j.agwat.2021.107299

Brocca, L., Tarpanelli, A., Filippucci, P., Dorigo, W., Zaussinger, F., Gruber, A., & Fernández-Prieto, D. (2018). How much water is used for irrigation? A new approach exploiting coarse resolution satellite soil moisture products. *International Journal of Applied Earth Observation and Geoinformation*, *73*, 752–766. https://doi.org/10.1016/j.jag.2018.08.023

Brodzik, M. J., Billingsley, B., Haran, T., Raup, B., & Savoie, M. H. (2012). EASE-Grid 2.0: Incremental but Significant Improvements for Earth-Gridded Data Sets. *ISPRS International Journal of Geo-Information*, *1*(1), 32–45. https://doi.org/10.3390/ijgi1010032

Brombacher, J., Silva, I. R. de O., Degen, J., & Pelgrum, H. (2022). A novel evapotranspiration based irrigation quantification method using the hydrological similar pixels algorithm. *Agricultural Water Management*, *267*, 107602. https://doi.org/10.1016/j.agwat.2022.107602

Chai, Q., Gan, Y., Zhao, C., Xu, H.-L., Waskom, R. M., Niu, Y., & Siddique, K. H. M. (2016). Regulated deficit irrigation for crop production under drought stress. A review. *Agronomy for Sustainable Development*, *36*(1), 3. https://doi.org/10.1007/s13593-015-0338-6

Campbell, G. S. (1974). A SIMPLE METHOD FOR DETERMINING UNSATURATED CONDUCTIVITY FROM MOISTURE RETENTION DATA. *Soil Science*, *117*(6), 311–314. https://journals.lww.com/soilsci/Fulltext/1974/06000/A_SIMPLE_METHOD_FO

Dari, J., Brocca, L., Quintana-Seguí, P., Escorihuela, M. J., Stefan, V., & Morbidelli, R. (2020). Exploiting High-Resolution Remote Sensing Soil Moisture to Estimate Irrigation Water Amounts over a Mediterranean Region. *Remote Sensing*, *12*(16), 2593. https://doi.org/10.3390/rs12162593

Dari, J., Quintana-Seguí, P., Morbidelli, R., Saltalippi, C., Flammini, A., Giugliarelli, E., Escorihuela, M. J., Stefan, V., & Brocca, L. (2022). Irrigation estimates from space: Implementation of different approaches to model the evapotranspiration contribution within a soil-moisture-based inversion algorithm. *Agricultural Water Management*, *265*, 107537. https://doi.org/10.1016/j.agwat.2022.107537

Das, N. N., Entekhabi, D., Dunbar, R. S., Kim, S., Yueh, S., Colliander, A., O'Neill, P. E., Jackson, T., Jagdhuber, T., Chen, F., Crow, W. T., Walker, J., Berg, A., Bosch, D., Caldwell, T., and Cosh, M. (2020). SMAP/Sentinel-1 L2 Radiometer/Radar 30-Second Scene 3 km EASE-Grid Soil Moisture, Version 3. Boulder, Colorado USA. NASA National Snow and Ice Data Center Distributed Active Archive Center. doi: https://doi.org/10.5067/ASB0EQO2LYJV.

Das, N. N., Entekhabi, D., Dunbar, R. S., Chaubell, M. J., Colliander, A., Yueh, S., Jagdhuber, T., Chen, F., Crow, W., O'Neill, P. E., Walker, J. P., Berg, A., Bosch, D. D., Caldwell, T., Cosh, M. H., Collins, C. H., Lopez-Baeza, E., & Thibeault, M. (2019). The SMAP and Copernicus Sentinel 1A/B microwave active-passive high resolution surface soil moisture product. *Remote Sensing of Environment*. https://doi.org/10.1016/j.rse.2019.111380.

Döll, P., & Siebert, S. (2002). Global modeling of irrigation water requirements. *Water Resources Research*, *38*(4), 8–10. https://doi.org/10.1029/2001WR000355

Döll, P., Müller Schmied, H., Schuh, C., Portmann, F. T., & Eicker, A. (2014).

Global-scale assessment of groundwater depletion and related groundwater abstractions: Combining hydrological modeling with information from well observations and GRACE satellites. *Water Resources Research*, *50*(7), 5698–5720. https://doi.org/10.1002/2014WR015595

Dong, J., Steele-Dunne, S. C., Judge, J., & van de Giesen, N. (2015). A particle batch smoother for soil moisture estimation using soil temperature observations. *Advances in Water Resources*, *83*, 111–122. https://doi.org/10.1016/j.advwatres.2015.05.017

Farg, E., Arafat, S. M., Abd El-Wahed, M. S., & EL-Gindy, A. M. (2012). Estimation of Evapotranspiration ETc and Crop Coefficient Kc of Wheat, in south Nile Delta of Egypt Using integrated FAO-56 approach and remote sensing data. *The Egyptian Journal of Remote Sensing and Space Science*, *15*(1), 83–89. https://doi.org/10.1016/j.ejrs.2012.02.001

Feldman, A., Gianotti, D., Dong, J., Akbar, R., Crow, W., McColl, K., Nippert, J., Tumber-Dávila, S. J., Holbrook, N. M., Rockwell, F., & et al. (2022). Satellites capture soil moisture dynamics deeper than a few centimeters and are relevant to plant water uptake. *Earth and Space Science Open Archive*, 16. https://doi.org/10.1002/essoar.10511280.1

Felfelani, F., Pokhrel, Y., Guan, K., & Lawrence, D. M. (2018). Utilizing SMAP Soil Moisture Data to Constrain Irrigation in the Community Land Model. *Geophysical Research Letters*, *45*(23), 12, 812–892, 902. https://doi.org/10.1029/2018GL080870

Foster, T., Mieno, T., & Brozović, N. (2020). Satellite-Based Monitoring of Irrigation Water Use: Assessing Measurement Errors and Their Implications for Agricultural Water Management Policy. *Water Resources Research*, *56*(11), e2020WR028378. https://doi.org/10.1029/2020WR028378

Frappart, F., & Ramillien, G. (2018). Monitoring Groundwater Storage Changes Using the Gravity Recovery and Climate Experiment (GRACE) Satellite Mission: A Review. *Remote Sensing*, *10*(6). https://doi.org/10.3390/rs10060829

Gordon, N. J., Salmond, D. J., & Smith, A. F. M. (1993). Novel approach to nonlinear/non-Gaussian Bayesian state estimation. *IEE Proceedings F Radar and Signal Processing*, *140*(2), 107. https://doi.org/10.1049/ip-f-2.1993.0015

Haddeland, I., Lettenmaier, D. P., & Skaugen, T. (2006). Effects of irrigation on the water and energy balances of the Colorado and Mekong river basins. *Journal of Hydrology*, *324*(1–4), 210–223. https://doi.org/10.1016/j.jhydrol.2005.09.028

Hengl, T., Mendes de Jesus, J., Heuvelink, G. B. M., Ruiperez Gonzalez, M., Kilibarda, M., Blagotić, A., Shangguan, W., Wright, M. N., Geng, X., Bauer-Marschallinger, B., Guevara, M. A., Vargas, R., MacMillan, R. A., Batjes, N. H., Leenaars, J. G. B., Ribeiro, E., Wheeler, I., Mantel, S., & Kempen, B. (2017). SoilGrids250m: Global gridded soil information based on machine learning. *PLOS ONE*, *12*(2), e0169748. https://doi.org/10.1371/journal.pone.0169748

Huffman, George. J., Stocker, E. F., Bolvin, D. T., Nelkin, E. J., & Jackson, T. (2019). *GPM IMERG Final Precipitation L3 1 day 0.1 degree x 0.1 degree V06*. NASA Goddard Earth Sciences Data and Information Services Center. https://doi.org/10.5067/GPM/IMERGDF/DAY/06

Jägermeyr, J., Gerten, D., Heinke, J., Schaphoff, S., Kummu, M., & Lucht, W. (2015). Water savings potentials of irrigation systems: global simulation of processes and linkages. *Hydrology and Earth System Sciences*, *19*(7), 3073–3091. https://doi.org/10.5194/hess-19-3073-2015

Jalilvand, E., Abolafia-Rosenzweig, R., Tajrishy, M., & Das, N. N. (2021). Evaluation of SMAP/Sentinel 1 High-Resolution Soil Moisture Data to Detect Irrigation Over Agricultural Domain. *IEEE Journal of Selected Topics in Applied Earth Observations and Remote Sensing*, *14*, 10733–10747. https://doi.org/10.1109/JSTARS.2021.3119228

Jalilvand, E., Tajrishy, M., Ghazi Zadeh Hashemi, S. A., & Brocca, L. (2019). Quantification of irrigation water using remote sensing of soil moisture in a semi-arid region. *Remote Sensing of Environment*, *231*, 111226. https://doi.org/10.1016/j.rse.2019.111226

Javadian, M., Behrangi, A., Gholizadeh, M., & Tajrishy, M. (2019). METRIC and WaPOR Estimates of Evapotranspiration over the Lake Urmia Basin: Comparative Analysis and Composite Assessment. *Water*, *11*(8), 1647. https://doi.org/10.3390/w11081647

Joodaki, G., Wahr, J., & Swenson, S. (2014). Estimating the human contribution to groundwater depletion in the Middle East, from GRACE data, land surface models, and well observations. *Water Resources Research*, *50*(3), 2679–2692. https://doi.org/https://doi.org/10.1002/2013WR014633

Karimi, P., Bastiaanssen, W. G. M., Molden, D., & Cheema, M. J. M. (2013). Basin-wide water accounting based on remote sensing data: an application for the Indus Basin. *Hydrology and Earth System Sciences*, *17*(7), 2473–2486. https://doi.org/10.5194/hess-17-2473-2013

Kumar, S. v., Peters-Lidard, C. D., Santanello, J. A., Reichle, R. H., Draper, C. S., Koster, R. D., Nearing, G., & Jasinski, M. F. (2015). Evaluating the utility of satellite soil moisture retrievals over irrigated areas and the ability of land data assimilation methods to correct for unmodeled processes. *Hydrology and Earth System Sciences*, *19*(11), 4463–4478. https://doi.org/10.5194/hess-19-4463-2015

Kumar, S. v., Reichle, R. H., Harrison, K. W., Peters-Lidard, C. D., Yatheendradas, S., & Santanello, J. A. (2012). A comparison of methods for a priori bias correction in soil moisture data assimilation. *Water Resources Research*, *48*(3). https://doi.org/10.1029/2010WR010261

Lawston, P. M., Santanello, J. A., & Kumar, S. v. (2017). Irrigation Signals Detected From SMAP Soil Moisture Retrievals. *Geophysical Research Letters*,

44(23), 11,860-11,867. https://doi.org/10.1002/2017GL075733

Lawston, P. M., Santanello Jr., J. A., Franz, T. E., & Rodell, M. (2017). Assessment of irrigation physics in a land surface modeling framework using non-traditional and human-practice datasets. *Hydrology and Earth System Sciences*, *21*(6), 2953–2966. https://doi.org/10.5194/hess-21-2953-2017

Leng, G., Huang, M., Tang, Q., Gao, H., & Leung, L. R. (2014). Modeling the Effects of Groundwater-Fed Irrigation on Terrestrial Hydrology over the Conterminous United States. *Journal of Hydrometeorology*, *15*(3), 957–972. https://doi.org/10.1175/JHM-D-13-049.1

Leng, G., Leung, L. R., & Huang, M. (2017). Significant impacts of irrigation water sources and methods on modeling irrigation effects in the ACME Land Model. *Journal of Advances in Modeling Earth Systems*, *9*(3), 1665–1683. https://doi.org/https://doi.org/10.1002/2016MS000885

Liang, X., Lettenmaier, D. P., Wood, E. F., & Burges, S. J. (1994). A simple hydrologically based model of land surface water and energy fluxes for general circulation models. *Journal of Geophysical Research*, *99*(D7), 14415. https://doi.org/10.1029/94JD00483

Massari, C., Modanesi, S., Dari, J., Gruber, A., de Lannoy, G. J. M., Girotto, M., Quintana-Seguí, P., le Page, M., Jarlan, L., Zribi, M., Ouaadi, N., Vreugdenhil, M., Zappa, L., Dorigo, W., Wagner, W., Brombacher, J., Pelgrum, H., Jaquot, P., Freeman, V., … Brocca, L. (2021). A Review of Irrigation Information Retrievals from Space and Their Utility for Users. *Remote Sensing*, *13*(20), 4112. https://doi.org/10.3390/rs13204112

McColl, K. A., Alemohammad, S. H., Akbar, R., Konings, A. G., Yueh, S., & Entekhabi, D. (2017). The global distribution and dynamics of surface soil moisture. *Nature Geoscience*, *10*(2), 100–104. https://doi.org/10.1038/ngeo2868

McColl, K. A., Wang, W., Peng, B., Akbar, R., Short Gianotti, D. J., Lu, H., Pan, M., & Entekhabi, D. (2017). Global characterization of surface soil moisture drydowns. *Geophysical Research Letters*, *44*(8), 3682–3690. https://doi.org/10.1002/2017GL072819

Modanesi, S., Massari, C., Bechtold, M., Lievens, H., Tarpanelli, A., Brocca, L., Zappa, L., & de Lannoy, G. J. M. (2022). Challenges and benefits of quantifying irrigation through the assimilation of Sentinel-1 backscatter observations into Noah-MP. *Hydrology and Earth System Sciences Discussions*, *2022*, 1–31. https://doi.org/10.5194/hess-2022-61

Modanesi, S., Massari, C., Gruber, A., Lievens, H., Tarpanelli, A., Morbidelli, R., & de Lannoy, G. J. M. (2021). Optimizing a backscatter forward operator using Sentinel-1 data over irrigated land. *Hydrology and Earth System Sciences*, *25*(12), 6283–6307. https://doi.org/10.5194/hess-25-6283-2021

Moradkhani, H., Hsu, K.-L., Gupta, H., & Sorooshian, S. (2005). Uncertainty assessment of hydrologic model states and parameters: Sequential

data assimilation using the particle filter. *Water Resources Research*, *41*(5). https://doi.org/10.1029/2004WR003604

Mousivand, A., Mirzapour, F., Azadbakht, M., Mousivand, Y., Babaei, H., Sima, S., Darvishi Boloorani, A., Iannini, L., GhasemiNik, F., & Cheraghi, K. (2020). Collaborative Crop Mapping of the Urmia Lake Basin, Iran, FAO/Urmia Lake Restoration Program (ULRP) joint project.

Ozdogan, M., Rodell, M., Beaudoing, H. K., & Toll, D. L. (2010). Simulating the Effects of Irrigation over the United States in a Land Surface Model Based on Satellite-Derived Agricultural Data. *Journal of Hydrometeorology*, *11*(1), 171–184. https://doi.org/10.1175/2009JHM1116.1

Parsinejad, M., Rosenberg, D. E., Ghale, Y. A. G., Khazaei, B., Null, S. E., Raja, O., Safaie, A., Sima, S., Sorooshian, A., & Wurtsbaugh, W. A. (2022). 40-years of Lake Urmia restoration research: Review, synthesis and next steps. *Science of The Total Environment*, *832*, 155055. https://doi.org/10.1016/j.scitotenv.2022.155055

Pokhrel, Y., Hanasaki, N., Koirala, S., Cho, J., Yeh, P. J.-F., Kim, H., Kanae, S., & Oki, T. (2012). Incorporating Anthropogenic Water Regulation Modules into a Land Surface Model. *Journal of Hydrometeorology*, *13*(1), 255–269. https://doi.org/10.1175/JHM-D-11-013.1

Pokhrel, Y. N., Hanasaki, N., Wada, Y., & Kim, H. (2016). Recent progresses in incorporating human land–water management into global land surface models toward their integration into Earth system models. *WIREs Water*, *3*(4), 548–574. https://doi.org/10.1002/wat2.1150

Rodell, M., Houser, P. R., Jambor, U., Gottschalck, J., Mitchell, K., Meng, C.-J., Arsenault, K., Cosgrove, B., Radakovich, J., Bosilovich, M., Entin, J. K., Walker, J. P., Lohmann, D., & Toll, D. (2004). The Global Land Data Assimilation System. *Bulletin of the American Meteorological Society*, *85*(3), 381–394. https://doi.org/10.1175/BAMS-85-3-381

Sadri, S., Famiglietti, J. S., Pan, M., Beck, H. E., Berg, A., & Wood, E. F. (2022). FarmCan: A Physical, Statistical, and Machine Learning Model to Forecast Crop Water Deficit at Farm Scales. *Hydrology and Earth System Sciences Discussions*, *2022*, 1–32. https://doi.org/10.5194/hess-2022-96

Saxton, K. E., & Rawls, W. J. (2006). Soil Water Characteristic Estimates by Texture and Organic Matter for Hydrologic Solutions. *Soil Science Society of America Journal*, *70*(5), 1569–1578. https://doi.org/10.2136/sssaj2005.0117

Scanlon, B. R., Faunt, C. C., Longuevergne, L., Reedy, R. C., Alley, W. M., McGuire, V. L., & McMahon, P. B. (2012). Groundwater depletion and sustainability of irrigation in the US High Plains and Central Valley. Proceedings of the National Academy of Sciences, 109(24), 9320–9325. https://doi.org/10.1073/pnas.1200311109

Schulz, S., Darehshouri, S., Hassanzadeh, E., Tajrishy, M., & Schüth, C. (2020). Climate change or irrigated agriculture – what drives the water level decline of Lake Urmia. *Scientific Reports*, *10*(1), 236. https://doi.org/10.1038/s41598-019-57150-y

Shadkam, S., Ludwig, F., van Oel, P., Kirmit, Ç., & Kabat, P. (2016). Impacts of climate change and water resources development on the declining inflow into Iran's Urmia Lake. *Journal of Great Lakes Research*, *42*(5), 942–952. https://doi.org/10.1016/j.jglr.2016.07.033

Shah, T. (2014). *Groundwater governance and irrigated agriculture*. Global Water Partnership (GWP) Stockholm.

Sima, S., Rosenberg, D. E., Wurtsbaugh, W. A., Null, S. E., & Kettenring, K. M. (2021). Managing Lake Urmia, Iran for diverse restoration objectives: Moving beyond a uniform target lake level. *Journal of Hydrology: Regional Studies*, 35, 100812. https://doi.org/10.1016/j.ejrh.2021.100812

Sorooshian, S., Li, J., Hsu, K., & Gao, X. (2011). How significant is the impact of irrigation on the local hydroclimate in California's Central Valley? Comparison of model results with ground and remote-sensing data. *Journal of Geophysical Research*, *116*(D6), D06102. https://doi.org/10.1029/2010JD014775

Steffen, W., Richardson, K., Rockström, J., Cornell, S. E., Fetzer, I., Bennett, E. M., Biggs, R., Carpenter, S. R., de Vries, W., de Wit, C. A., Folke, C., Gerten, D., Heinke, J., Mace, G. M., Persson, L. M., Ramanathan, V., Reyers, B., & Sörlin, S. (2015). Planetary boundaries: Guiding human development on a changing planet. *Science*, *347*(6223), 1259855. https://doi.org/10.1126/science.1259855

van Eekelen, M. W., Bastiaanssen, W. G. M., Jarmain, C., Jackson, B., Ferreira, F., van der Zaag, P., Saraiva Okello, A., Bosch, J., Dye, P., Bastidas-Obando, E., Dost, R. J. J., & Luxemburg, W. M. J. (2015). A novel approach to estimate direct and indirect water withdrawals from satellite measurements: A case study from the Incomati basin. *Agriculture, Ecosystems & Environment*, *200*, 126–142. https://doi.org/10.1016/j.agee.2014.10.023

Weerts, A. H., & el Serafy, G. Y. H. (2006). Particle filtering and ensemble Kalman filtering for state updating with hydrological conceptual rainfall-runoff models. *Water Resources Research*, *42*(9). https://doi.org/10.1029/2005WR004093

Wells, O. D. (2015). *Rising Stakes: Towards Sustainable Agricultural Ground-Water Use*. OECD: Paris, France.

Wester, P., Hoogesteger, J., & Vincent, L. (2009). Local IWRM organizations for groundwater regulation: The experiences of the Aquifer Management Councils (COTAS) in Guanajuato, Mexico. *Natural Resources Forum*, *33*(1), 29–38. https://doi.org/10.1111/j.1477-8947.2009.01206.x

World Bank. (2020). *Water in Agriculture*.

Zaman, M. R., Morid, S., & Delavar, M. (2016). Evaluating climate adaptation strategies on agricultural production in the Siminehrud catchment and inflow into Lake Urmia, Iran using SWAT within an OECD framework. *Agricultural Systems*, *147*, 98–110.

Zaussinger, F., Dorigo, W., Gruber, A., Tarpanelli, A., Filippucci, P., & Brocca, L. (2019). Estimating irrigation water use over the contiguous United States by combining satellite and reanalysis soil moisture data. *Hydrology and Earth System Sciences*, *23*(2), 897–923. https://doi.org/10.5194/hess-23-897-2019

Zhang, J., Guan, K., Peng, B., Jiang, C., Zhou, W., Yang, Y., Pan, M., Franz, T. E., Heeren, D. M., & Rudnick, D. R. (2021). Challenges and opportunities in precision irrigation decision-support systems for center pivots. *Environmental Research Letters*, *16*(5), 053003.

Zhou, J., Wu, Z., Crow, W. T., Dong, J., & He, H. (2020). Improving Spatial Patterns Prior to Land Surface Data Assimilation via Model Calibration Using SMAP Surface Soil Moisture Data. *Water Resources Research*, *56*(10), e2020WR027770. https://doi.org/10.1029/2020WR027770